

# Molecular Dynamics of Water in Wood Studied by Fast Field Cycling Nuclear Magnetic Resonance Relaxometry

Xinyu Li, Ximing Wang, and Minghui Zhang \*

Water plays a very important role in wood and wood products. The molecular motion of water in wood is susceptible to thermal activation. Thermal energy makes water molecules more active and weakens the force between water and wood; therefore, the water molecules dynamic properties are greatly influenced. Molecular dynamics study is important for wood drying; this paper therefore focuses on water molecular dynamics in wood through fast field cycling nuclear magnetic resonance relaxometry techniques. The results show that the spin-lattice relaxation rate decreases with the Larmor frequency. Nuclear magnetic resonance dispersion profiles at different temperatures could separate the relaxation contribution of water in bigger pores and smaller pores. The  $T_1$  distribution from wide to narrow at 10 MHz Larmor frequency reflects the shrinkage of pore size with the higher temperature. The dependence of spin-lattice relaxation rate on correlation time for water molecular motion based on BPP (proposed by Bloembergen, Purcell, and Pound) theory shows that water correlation time increases with higher temperature, and its activation energy, calculated using the Arrhenius transformation equation, is  $9.06 \pm 0.53$  kJ/mol.

**Keywords:** Molecular dynamics; Fast field cycling nuclear magnetic resonance relaxometry; Nuclear magnetic resonance dispersion profile; Correlation time; Activation energy; Wood

**Contact information:** College of Materials Science and Art Design, Inner Mongolia Agricultural University, Hohhot 010018, China; \*Corresponding author: zhangminghui@imau.edu.cn

## INTRODUCTION

Fast field cycling nuclear magnetic resonance relaxometry (FFC-NMR), often called nuclear magnetic resonance dispersion (NMRD), is a powerful tool for studying dynamics in polymers and liquids (Kimmich and Ansaldo 2004). The dynamic properties of molecular systems are traditionally determined by nuclear magnetic resonance techniques through the measurement of spin-lattice relaxation rates ( $R_1$ ) (Keeler 2005). FFC-NMR is sensitive to a wide range of molecular motion (Badea *et al.* 2014).

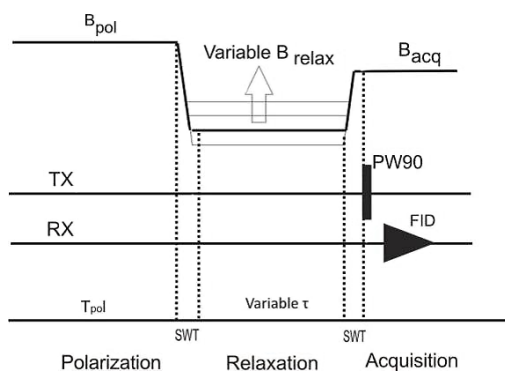


**Fig. 1a.** Polarized sequence

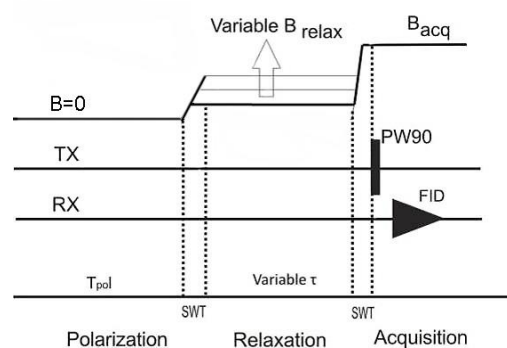


**Fig. 1b.** Non-polarized sequence

FFC-NMR is based on the cycling of the magnetic field through three different values: the polarization ( $B_{\text{pol}}$ ), relaxation ( $B_{\text{relax}}$ ), and acquisition ( $B_{\text{acq}}$ ) fields (Kimmich and Anordo 2004).  $B_{\text{pol}}$  is applied only for a polarized sequence (Fig. 1a.) to achieve magnetization saturation by polarization. Then, the magnetic field is quickly switched to  $B_{\text{relax}}$  for a period ( $\tau$ ), during which the intensity of the magnetization changes to reach a new equilibrium condition (relaxation). Finally, the magnetization changes are observed at  $B_{\text{acq}}$  following the acquisition of free induction decay (FID). Similarly, a non-polarized sequence (Fig. 1b.) is also divided into three steps; the only difference is that there is no need to polarize ( $B_{\text{pol}}=0$ ) when relaxation progress occurs at high  $B_{\text{relax}}$  fields. The spin-lattice relaxation rate ( $R_1$ ) is obtained at each fixed  $B_{\text{relax}}$  value through a progressive variation of the  $\tau$  values and is usually called the NMRD profile.

FFC-NMR exhibits good performance, not only in homogeneous molecular systems, but also in complex systems. It is a rich source of dynamic information over a large range of length scales, from localized and fast motions at large frequency to delocalized and slow motions at low frequency (Korb *et al.* 2013). The multi-component relaxometry properties of leaves and leaf-litters have been confirmed by FFC-NMR; the results indicate that relaxation mechanisms of degenerated leaf-litters and undecomposed leaves can be distinguished by their various segmental motion contributions (Berns *et al.* 2011). An investigation of the gray cement hydration process with FFC-NMR shows that the surface and bulk contributions from the global measured relaxation rate can be well separated (Badea *et al.* 2014). Conte *et al.* (2009b) found that the  $R_1$  of cellulose-bound phosphoric acid ranges from a maximum of approximately  $400 \text{ s}^{-1}$  down to  $50 \text{ s}^{-1}$  in the NMRD profile.

In 2009, FFC-NMR relaxometry was applied to plant tissue for the first time (Conte *et al.* 2009a). In addition, it has also been used for investigating the water dynamics of biochars (Pasquale *et al.* 2012). To our knowledge, relaxation of water in wood has been investigated broadly with conventional NMR relaxometry (Araujo *et al.* 1992; Telkki *et al.* 2013), but without FFC-NMR. So the goal of this study was to apply FFC-NMR for the assessment of the relaxation properties of water in wood.

## EXPERIMENTAL

### Materials

Cylindrical sapwood samples with diameters of approximately 6 mm and lengths (longitudinal direction) of 20 mm were cut from green Qingpi poplar (*Populus platyphylla* var. *glauca*), which was harvested in Hohhot, China with an approximate age of 10 years.

### Methods

Before the FFC-NMR measurements, wood samples were weighed and then soaked with carbon tetrachloride in a standard 10-mm glass tube to greatly decrease the amount of water diffusion during the experiment. In addition, a Teflon® bar was put into the glass tube to ensure the sample remained submerged in carbon tetrachloride.

NMRD profiles were acquired on a SMARtracer FFC Relaxometer (Stelar s.r.l., Mede, PV, Italy) at 30, 40, 50, and 60 °C. The polarized sequence was applied when the relaxation magnetic fields were in the range of the proton Larmor frequencies between 0.01 and 3.5 MHz, the proton spins were polarized at a polarization field ( $B_{\text{pol}}$ ) corresponding to a Larmor frequency of 8 MHz for a period of polarization ( $T_{\text{pol}}$ ) at this frequency, 1 s

was used at present study. Furthermore, the non-polarized sequence was applied when the relaxation magnetic fields were in the range of the proton Larmor frequencies between 3.5 and 10 MHz. The relaxation magnetic fields were automatically switched from 10 MHz to 0.01 MHz for one NMRD profile with a program called NMRD Profile Wizard, which was embedded in the instrument's software (Stelar s.r.l., Mede, PV, Italy), and the measured value of relaxation field in the range 10 to 0.01 MHz for a period  $\tau$  varied on 32 logarithmic spaced time sets. FIDs were recorded following a single  $90^\circ$ ,  $4.5 \mu\text{s}$  pulse applied at an acquisition field corresponding to the proton Larmor frequency of 7.20 MHz. A time domain of  $50 \mu\text{s}$  sampled with 500 points was applied. The global FFC magnet-switching time was 2 ms, while the dead time was  $28 \mu\text{s}$ . A recycle delay of 3 s and scan number of 2 were always used.

The decay/recovery curves at each relaxation field were fitted using a first-order exponential decay/recovery function with the instrument's software. The NMRD profile fitting results were used for subsequent analysis and calculation.

## RESULTS AND DISCUSSION

### NMRD Profiles of Water in Wood

Wood is a kind of non-homogeneous porous material. Free water can move from one place to another in big pores, such as cell lumens. Such movement includes translational motion and rotational motion. Bound water combines tightly with hydroxyl groups in smaller pores, such as cell walls, and this hinders the water movement. Molecular motion fluctuates in magnetic fields and causes nuclear relaxation (Bakmutov 2004). The contribution to water relaxation in wood is due to intermolecular dipole-dipole interactions, which includes the dipole interaction between two water molecules and the dipole interaction between water molecules and hydroxyls, namely, the dipole interactions of free water and the dipole interactions of bound water.

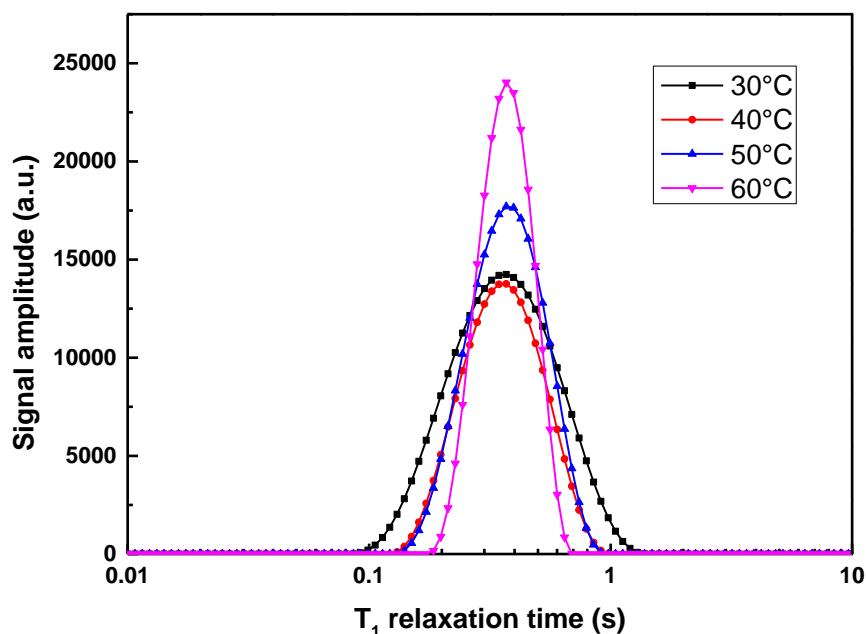


**Fig. 2.**  $T_1$  relaxation time distribution of water in wood obtained at Larmor frequency of 10 MHz at 30, 40, 50, and 60 °C

The original  $T_1$  data is only inverted at 10 MHz by the CONTIN (Provencher 1982) algorithm, which was due to the larger NMR sensitivity at this frequency as compared to the other proton Larmor frequencies (Kimmich and Anorado 2004). The inversion result shown in Fig. 2 indicates that there was only one water component determined by FFC-NMR. The  $T_1$  relaxation time distribution from wide to narrow reflects the shrinkage of pore size with the higher temperature. It is certain that the primary contribution to nuclear relaxation is due to free water, since the moisture content of sample is as much as 190.7% and bound water is tightly bound with hydroxyl groups in cell walls.

NMRD was employed to measure  $R_1$  at 30, 40, 50, and 60 °C. The resulting  $R_1$  values are shown in Table 1.

**Table 1.** NMRD Data of Water in Wood at 30, 40, 50, and 60 °C

Larmor frequency (MHz)	Spin-lattice relaxation rate (s <sup>-1</sup> )			
	30 °C	40 °C	50 °C	60 °C
9.9993	2.7994	2.6557	2.6643	2.7179
7.8803	2.9212	2.7927	2.8208	2.8501
6.2108	2.9513	2.9789	3.0501	3.0509
4.8937	3.0818	3.2455	3.2658	3.0593
3.8572	3.5248	3.4494	3.3630	3.5439
3.0397	4.0619	3.8831	4.0294	4.0579
2.3946	4.6158	4.3801	4.5640	4.4221
1.8874	5.1024	5.1125	4.8396	4.9817
1.4869	5.3227	5.6284	5.5205	5.5693
1.1717	5.7392	6.0269	6.2268	6.0303
0.9235	6.3061	6.5435	6.6366	6.7645
0.7276	6.8039	6.9122	7.0257	7.4158
0.5734	7.4821	7.3538	7.8862	8.1973
0.4522	7.8758	7.8959	8.4617	9.0095
0.3560	8.0892	8.5711	9.2177	10.1756
0.2807	9.0562	9.3960	9.9071	10.3998
0.2212	9.3265	10.1450	10.8940	11.4320
0.1742	9.9109	10.6220	11.6050	12.5460
0.1372	10.8860	11.5390	12.2050	12.6230
0.1082	11.8930	12.4200	12.6230	13.4220
0.0854	12.7610	12.7260	13.6640	14.6840
0.0672	13.2220	13.6730	14.2400	14.9300
0.0530	13.3270	13.9260	15.0340	16.3260
0.0417	14.2480	14.6250	16.0260	17.2800
0.0329	15.1290	15.8290	16.8410	17.8530
0.0259	15.9190	16.3340	18.0300	18.9710
0.0205	16.0810	17.1910	18.4550	19.9610
0.0161	17.1080	18.3860	19.0420	21.0160
0.0127	17.3570	18.5100	20.0530	21.4320
0.0100	17.6740	19.0370	20.7440	22.5710

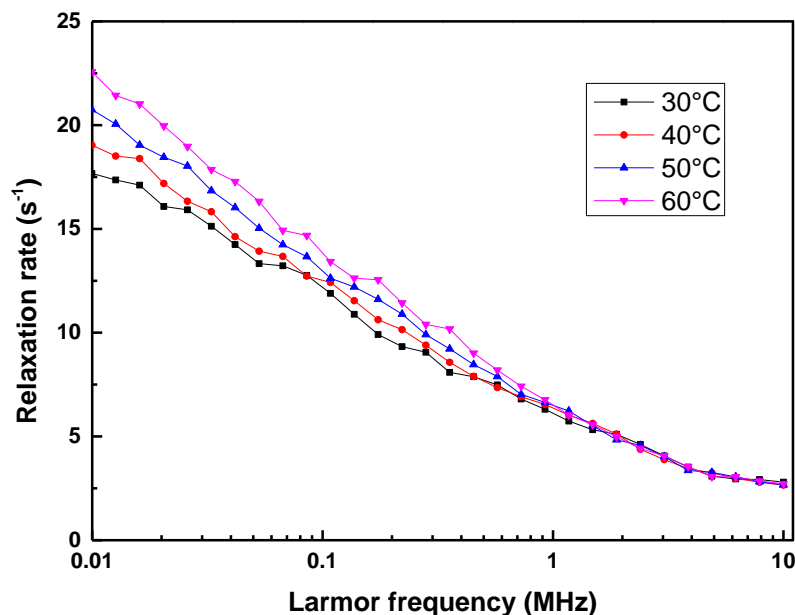


Fig. 3. NMRD profiles for water in wood at 30, 40, 50, and 60 °C

All the nuclear Larmor frequencies are affected by the applied magnetic field. For this reason, only the molecular motions oscillating at the frequency of the specific magnetic field value are effective in promoting nuclear relaxation. The same motions could not be effective for a different value of the applied magnetic field. Molecular motions strongly affect dipolar interactions (Conte and Alonzo 2013). The faster the motions are, the lower is the dipolar interaction efficiency, thereby favoring longer  $T_1$  values and shorter  $R_1$  values. Conversely, slower molecular dynamics can be associated with shorter spin–lattice relaxation times because of stronger nuclear dipolar interactions (Bakmutov 2004).

For wood, the bigger pores allow faster water motion. The fluctuant duration that gives rise to nuclear relaxation is longer because of the weak  $^1\text{H}$  dipole-dipole interactions and slower relaxation efficiency. This results in bigger  $T_1$  values and smaller  $R_1$  values. On the other hand, water in smaller pores is combined tightly with the wood matrix. In this situation the water movement is hindered because of strong  $^1\text{H}$  dipole-dipole interactions. The energy transition between fluctuant water proton spins and its surrounding is fast and hence promotes higher relaxation efficiency. As a result, the higher  $R_1$  values are observed. Therefore, the NMRD profile in Fig. 3 reflects the water relaxation properties in different pore sizes. The water motion is more hindered in smaller pores, such that strong  $^1\text{H}$  dipolar interaction results in bigger  $R_1$ ; however, the increscent effect in wood pore size promotes faster water motions. This lowers the  $^1\text{H}$  dipolar interaction strengths, and small  $R_1$  is achieved.

The increasing temperature had different influences on  $R_1$  at the whole Larmor frequencies. The unchanged  $R_1$  at higher Larmor frequencies ( $>2$  MHz) indicates that the water mobility in bigger pores is not influenced by the higher temperature. On the other hand, the increasing  $R_1$  at lower Larmor frequencies ( $<2$  MHz) reveals the water diffusion process in wood. The water molecules that are loosely combined with wood in bigger pores are easily being removed and diffuse into smaller pores by thermal energy. In this case, water migration will change the pore size. The non-homogeneous pore distribution tends to become more homogeneous, just as shown in Fig. 2. Additionally, the water migration

also leads to water mobility change. Water transform from big pores into small pores will reduce the water mobility, resulting in an increment of dipole interactions. In fact, the higher temperature, the more moisture migration, also the stronger will be the dipole interactions. Therefore, the higher temperature eliminates the weak dipolar interactions and also consolidates the strong dipolar interactions. As a consequence, higher  $R_1$  values are observed.

### Correlation Time ( $\tau_c$ ) of Water

The  $R_1$  relaxation contribution is described by the well-known BPP theory. The proton longitudinal relaxation rate is related to the spectral density function by the following equation (Pasquale *et al.* 2012),

$$R_1 = \alpha + \beta[0.2J(\omega_0) + 0.8J(2\omega_0)] \quad (1)$$

where  $\alpha$  represents the high-field relaxation rate, and  $\beta$  is a constant related to the dipolar interactions. The spectral density function  $J(\omega_0)$  describes the distribution of the motion frequencies in a molecular system,

$$J(\omega_0) = \frac{\sum c_i \frac{\tau_{ci}}{1 + (\omega_0\tau_{ci})^2}}{\sum c_i} \quad (2)$$

where  $c_i$  is a fitting parameter,  $\tau_{ci}$  is the  $i^{\text{th}}$  correlation time, and  $\omega_0$  is the Larmor frequency.

The combination of Eqs. 1 and 2 provides a set of parameters  $\{c_i, \tau_{ci}\}$ , which are used to calculate the average correlation time ( $\langle\tau_c\rangle$ ) in the form (Halle *et al.* 1998),

$$\langle\tau_c\rangle = \frac{\sum_i c_i \tau_{ci}}{\sum_i c_i} \quad (3)$$

In this study,  $i = 1, 2, 3$  are used for the mathematical fit of the NMRD profiles. The average correlation time is obtained by combining Eqs 1 to 3.

Table 2 reports calculated values of  $\alpha$ ,  $\beta$ , and  $\langle\tau_c\rangle$ . The calculation results are reasonable in comparison with previous research of water motion on biochars (Pasquale *et al.* 2012).

**Table 2.** Water  $\tau_c$  at 30, 40, 50, and 60 °C

Temperature(°C)	$\alpha$ (s <sup>-1</sup> )	$\beta$ (×10 <sup>6</sup> s <sup>-2</sup> )	$\langle\tau_c\rangle$ (×10 <sup>-6</sup> s <sup>-1</sup> )
30	2.35±0.2	4.51±0.2	0.80±0.05
40	2.38±0.1	4.81±0.1	0.89±0.02
50	2.47±0.1	4.99±0.1	0.98±0.03
60	2.56±0.2	5.08±0.2	1.11±0.03

In general, the shorter  $\alpha$  and  $\beta$  value, the weaker dipolar interactions, and also the less constrained are the water molecules to the porous media. On the other hand, the higher  $\alpha$  and  $\beta$  value, the stronger dipolar interactions, and also the tighter are the water molecules bound to matrix (Pasquale *et al.* 2012). The increment of  $\alpha$  and  $\beta$  in Table 2 indicates that higher temperature increases water dipolar interactions. Actually, the higher temperature

makes the looser water in big pores diffuse into small pores, and thus the weaker dipolar interactions of water will become stronger. Hence, the higher  $\alpha$  and  $\beta$  values are obtained.

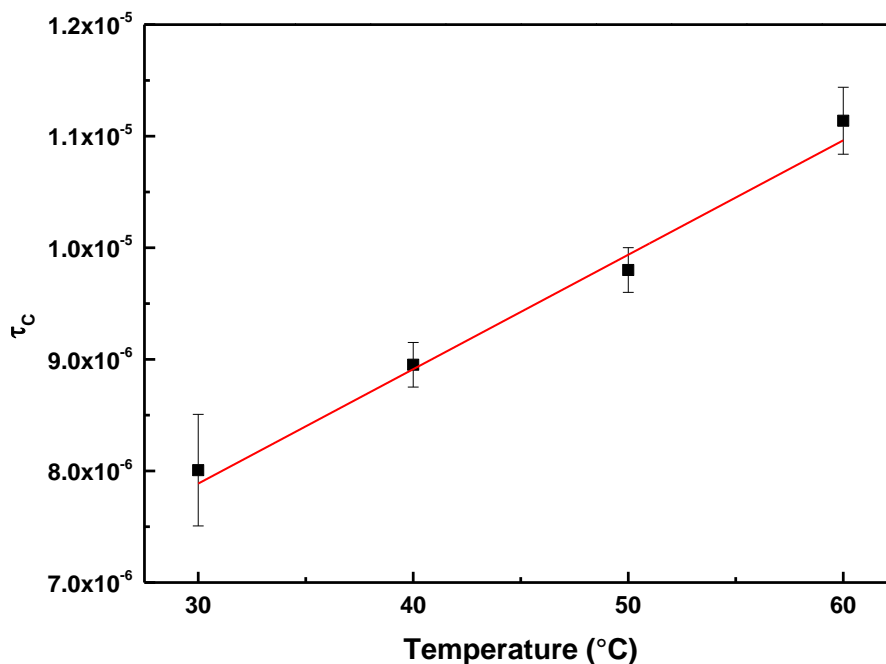


Fig. 4.  $\tau_c$  for water in wood at 30, 40, 50, and 60 °C. The red line is the best fit of  $\tau_c$

The quantity  $\tau_c$  is a measure of the time needed for molecular reorientation in system. The longer the  $\tau_c$  value, the slower will be the molecular motions, and the molecule motion will be restricted. Conversely, the shorter the  $\tau_c$  values, the faster will be the molecular motions due to higher degrees of freedom in larger spaces. Figure 4 shows that  $\tau_c$  is linearly increasing with the temperature. This indicates that at the higher temperature, water migrates from bigger pores into the smaller ones, and the pore shrinkage reduces the water mobility.

### Activation Energy ( $E_a$ ) of Water

$E_a$  is an important parameter in molecular dynamics. In chemistry, it describes the minimum energy that must be available to a chemical system with potential reactants to result in a chemical reaction. In other fields, it may also be defined as the minimum energy required to start a reaction. Generally, it reflects the bonding strength between substance and matrix. Therefore, the calculation of water  $E_a$  is also important for studying the force between water and wood and is important for wood drying.

The diffusion constants  $D$  are often used for characterization of molecular motions instead of  $\tau_c$  (Bakmutov 2004). Equation 2 is applied as follows (Chumakova *et al.* 2010),

$$D = \frac{\tau_c}{6} \quad (4)$$

A linear dependence between rotational diffusion constants and  $1/T$  indicates an Arrhenius relationship (Leezenberg *et al.* 1996),

$$D = D_0 \exp\left(-\frac{E_a}{RT}\right) \quad (5)$$

where  $D_0$  is a temperature-independent exponential factor,  $E_a$  is the activation energy, and  $R$  is the gas constant (8.3143 J/mol·K).

Linearizing Eq. 5,

$$\ln D = \ln D_0 - \frac{E_a}{RT} \quad (6)$$

The relationship between  $\tau_c$  and temperature conforms to Eqs. 5 and 6. The water  $E_a$  value calculated from the slope of Eq. 6 is  $9.06 \pm 0.53$  kJ/mol. It is smaller than the previous free water  $E_a$  calculation for redwood sapwood, 19.95 kJ/mol (Araujo *et al.* 1993). However, many factors have to be taken into consideration. Differences in wood species and experiment conditions can account for this disparity. It follows that the  $E_a$  calculation is reasonable.

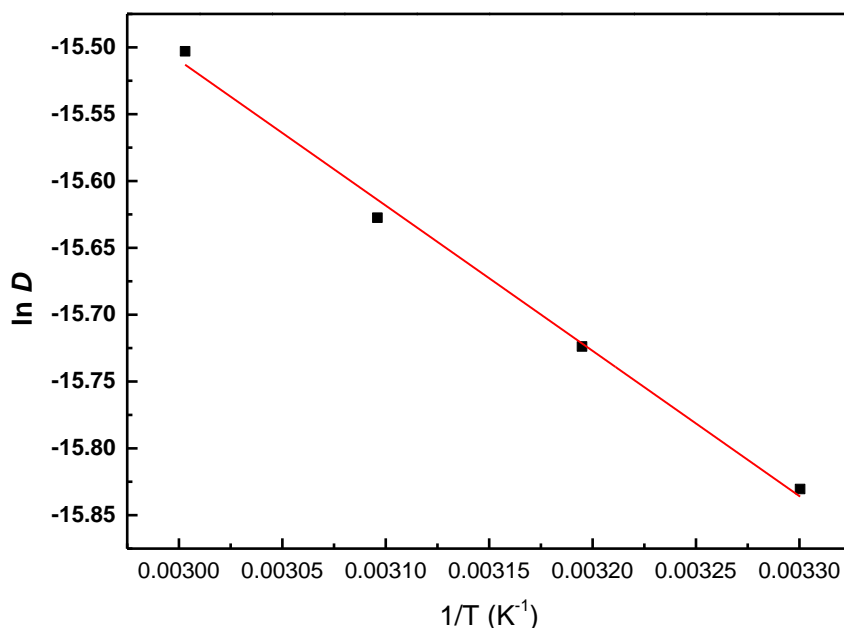


**Fig. 5.** The logarithm of diffusion constants ( $\ln D$ ) versus reciprocal of absolute temperature ( $1/T$ ). The red line is the best fit.

## CONCLUSIONS

1. Fast field cycling nuclear magnetic resonance relaxometry (FFC-NMR) can characterize the molecular dynamics of water in wood. The nuclear magnetic resonance dispersion (NMRD) profile can distinguish the water relaxation properties in different pore sizes; two molecular dynamics parameters, correlation time  $\tau_c$  and energy of activation  $E_a$ , can reflect the influence of temperature on water dynamics.
2. The inversion results by CONTIN at 10MHz indicated that higher temperature makes the wide range of pore distribution become smaller and more homogenous.

3. From a single NMRD profile, the lower  $R_1$  at higher Larmor frequencies is associated with water relaxation properties in bigger pores, while the higher  $R_1$  at lower Larmor frequencies is associated with water relaxation properties in smaller pores.
4. The NMRD profiles indicate that water transformation prompted by higher temperature decreases water mobility but increases the water dipole interactions.
5. The dependence of the spin-lattice relaxation rate ( $R_1$ ) on  $\tau_c$  for water molecular motion shows that higher temperature increases water  $\tau_c$ , and the water  $E_a$  is  $9.06 \pm 0.53$  kJ/mol.

## ACKNOWLEDGMENTS

This research is supported by the National Natural Science Foundation of China (30800866/ C1603 and 31160141/ C1603).

## REFERENCES CITED

- Araujo, C. D., MacKay, A. L., Hailey, J. R. T., Whittall, K. P., and Le, H. (1992). "Proton magnetic resonance techniques for characterization of water in wood: Application to white spruce," *Wood Science and Technology* 26(2), 101-113. DOI: 10.1007/BF00194466
- Araujo, C. D., Mackay, A. L., Whittall, K. P., and Hailey, J. R. T. (1993). "A diffusion model for spin-spin relaxation of compartmentalized water in wood," *Journal of Magnetic Resonance. Series B* 101(3), 248-261. DOI: 10.1006/jmrb.1993.1041
- Badea, C., Pop, A., Mattea, C., Stapf, S., and Ardelean, I. (2014). "The effect of curing temperature on early hydration of gray cement via fast field cycling-NMR relaxometry," *Applied Magnetic Resonance* 45(12), 1299-1309. DOI: 10.1007/s00723-014-0565-z
- Bakmutov, V. I. (2004). *Practical NMR Relaxation for Chemists*, John Wiley & Sons Ltd., Chichester, UK.
- Berns, A. E., Bubici, S., Pasquale, C. D., Alonzo, G., and Conte, P. (2011). "Applicability of solid state fast field cycling NMR relaxometry in understanding relaxation properties of leaves and leaf-litters," *Organic Geochemistry* 42(8), 978-984. DOI: 10.1016/j.orggeochem.2011.04.006
- Chumakova, N. A., Pergushov, V. I., Vorobiev, A. K., and Kokorin, A. I. (2010). "Rotational and translational mobility of nitroxide spin probes in ionic liquids and molecular solvents," *Applied Magnetic Resonance* 39(4), 409-421. DOI: 10.1007/s00723-010-0177-1
- Conte, P., and Alonzo, G. (2013). "Environmental NMR: Fast-field-cycling relaxometry," *eMagRes* 2(3), 389-398. DOI: 10.1002/9780470034590.emrst1330
- Conte, P., Bubici, S., Palazzolo, E., and Alonzo, G. (2009a). "Solid-state  $^1\text{H}$ -NMR relaxation properties of the fruit of a wild relative of eggplant at different proton Larmor frequencies," *Spectroscopy Letters* 42(5), 235-239. DOI: 10.1080/00387010902895038
- Conte, P., Maccotta, A., Pasquale, C. D., Bubici, S., and Alonzo, G. (2009b). "Dissolution mechanism of crystalline cellulose in  $\text{H}_3\text{PO}_4$  as assessed by high-field

- NMR spectroscopy and fast field cycling NMR relaxometry,” *Journal of Agricultural and Food Chemistry* 57(19), 8748-8752. DOI: 10.1021/jf9022146
- Halle, B., Johannesson, H., and Venu, K. (1998). “Model-free analysis of stretched relaxation dispersions,” *Journal of Magnetic Resonance* 135(1), 1-13. DOI: 10.1006/jmre.1998.1534
- Keeler, J. (2005). *Understanding NMR spectroscopy*, Wiley, New York, NY.
- Kimmich, R., and Anordo, E. (2004). “Field-cycling NMR relaxometry,” *Progress in Nuclear Magnetic Resonance Spectroscopy* 44(3-4), 257-320. DOI: 10.1016/j.pnmrs.2004.03.002
- Korb, J.-P., Patural, L., Govin, A., and Grosseau, P. (2013). “NMR investigations of water retention mechanism by cellulose ethers in cement-based materials,” in: *Mechanics and Physics of Creep, Shrinkage, and Durability of Concrete*, Franz-Joseph, U., Hamlin, J. M., and Pellenq, R. J.-M. (eds.), American Society of Civil Engineers, Reston, VA, pp. 102-109. DOI: 10.1061/9780784413111.011
- Leezenberg, P. B., Marcus, A. H., Frank, C. W., and Fayer, M. D. (1996). “Rotational dynamics of naphthalene-labeled cross-link junctions in poly(dimethylsiloxane) elastomers,” *The Journal of Physical Chemistry* 100(18), 7646-7655. DOI: 10.1021/jp953632u
- Pasquale, C. D., Marsala, V., Berns, A. E., Valagussa, M., Pozzi, A., Alonzo, G., and Conte, P. (2012). “Fast field cycling NMR relaxometry characterization of biochars obtained from an industrial thermochemical process,” *Journal of Soils and Sediments* 12(8), 1211-1221. DOI: 10.1007/s11368-012-0489-x
- Provencher, S.W. (1982). “CONTIN: A general purpose constrained regularization program for inverting noisy linear algebraic and integral equations,” *Computer Physics Communications* 27(3), 229-242. DOI: 10.1016/0010-4655(82)90174-6
- Telkki, V.-V., Yliniemi, M., and Jokisaari, J. (2013). “Moisture in softwoods: Fiber saturation point, hydroxyl site content, and the amount of micropores as determined from NMR relaxation time distributions,” *Holzforschung* 67(3), 291-300. DOI: 10.1515/hf-2012-0057

Article submitted: September 22, 2015; Peer review completed: December 2, 2015;  
Revised version received: December 14, 2015; Accepted: December 15, 2015; Published:  
January 11, 2016.

DOI: 10.15376/biores.11.1.1882-1891